

Simplified Range-Separation Tuning as a Practical Starting Point for G_0W_0 and Bethe-Salpeter Calculations

Aditi Singh,^{1,*} Bogumiła Jezierska,¹ Subrata Jana,¹ and Szymon Śmiga^{1,†}

¹ Institute of Physics, Faculty of Physics, Astronomy and Informatics,
Nicolaus Copernicus University in Toruń, ul. Grudziądzka 5, 87-100 Toruń, Poland

(Dated: January 21, 2026)

The accuracy of one-shot G_0W_0 and the Bethe-Salpeter equation (BSE) is well known to be highly sensitive to the choice of the starting-point eigensystem, typically obtained from mean-field theory. A highly effective method explored is the use of density functional approximation (DFA) with a range-separated hybrid (RSH) approach. In this work, we evaluate the performance of G_0W_0 in predicting ionization potentials and the BSE for describing neutral excitations, employing a recently proposed, broadly applicable, and computationally efficient range-separation tuning scheme [Singh *et. al.*, Journal of Physical Chemistry Letters, 16, 32, 8198–8208, (2025)]. Our results demonstrate that this simplified tuning protocol provides an accurate starting point for many-body perturbation theory, thereby eliminating the need for conventional, multi-step optimally tuned RSH optimization procedure. The resulting quasiparticle energies from G_0W_0 closely reproduce reference ionization potentials, while BSE calculations based on the same tuned RSH orbitals yield quantitatively accurate optical absorption spectra and excitonic properties across a range of molecular systems and clusters.

INTRODUCTION

Computationally intensive many-body perturbation theory (MBPT) methods, particularly Green's function-based GW and Bethe-Salpeter equation (BSE) approaches, are now routinely applied to achieve high precision in predicting properties across molecules, clusters, and materials [8, 9, 31, 69, 75, 91, 102]. This progress is driven by significant advancements in computational software [2, 12, 16, 25, 72, 81, 87, 103, 104], scalable algorithms [1, 21, 22, 27, 30, 35, 46, 73, 78, 79, 93, 107, 112, 130–132, 135], and high-performance computing resources [6]. Although the underlying formalism of GW and BSE is in principle exact, practical implementations require approximations to reduce computational cost while maintaining predictive accuracy. Among them, the non-self-consistent GW (G_0W_0) [3, 13, 28, 32, 39–41, 47–49, 58, 61, 70, 74, 77, 83, 92, 100, 109, 113, 114, 122, 126–128, 136] and BSE@ G_0W_0 [40] approaches have emerged as valuable corrections to the shortcomings of standard density functional theory[14] (DFT) with approximate exchange-correlation (XC) functionals, particularly for ionization potentials (IP), band gaps, excitation energies, and exciton binding energies. However, the G_0W_0 results strongly depend on the quality of the starting-point eigensystem [11, 34, 97, 128, 141], which is typically obtained from Kohn-Sham DFT (KS-DFT) calculations with either semilocal or hybrid XC approximation [3, 13, 28, 32, 39, 41, 47, 58, 61, 70, 74, 77, 83, 92, 100, 109, 113, 114, 126–128, 136].

Semilocal functionals, although computationally inexpensive, are less favourable [11, 34, 141] due to several well-known deficiencies [31, 85, 94, 111, 128, 141]. Hybrid functionals, and particularly range-separated hybrid (RSH), partially mitigate these deficiencies [43, 44, 53–

57, 66]. RSH functionals introduce a physically motivated separation between short-range (sr) DFT exchange and long-range (lr) Hartree-Fock (HF) exchange, restoring the correct asymptotic $\sim -1/r$ in the exchange potential [38, 67, 95]. The combination of this correction with the optimal tuning of the range-separation parameter [64, 101] yields: (i) significant improvements in describing long-range charge transfer processes, giving accurate excitation energies within the time-dependent DFT (TDDFT) framework [17–19, 26, 37, 45, 52, 62, 76, 105, 108, 117, 142], (ii) provides reliable IP derived from the highest occupied molecular orbital (HOMO) [4, 59], and (iii) delivers accurate HOMO-LUMO or band gaps [20, 36, 51, 89, 138].

Usually, the RS tuning parameter is obtained by targeting a certain energy level or energy gap in the considered system[65, 101]. In the former scheme, one finds the ω value so that the HOMO orbital energy matches the first IP of the system, calculated as the energy difference between the neutral and the ionic species. We recall that for exact DFT calculations, the two computed quantities should be the same[120]. Although this kind of tuning yields accurate results, it requires multiple self-consistent field (SCF) evaluations for neutral and ionic systems and can occasionally fail. This situation can be particularly encountered in open-shell systems or species with near-degenerate frontier orbitals and molecules with unbound anionic state [60, 64, 98, 101, 121]. The challenge of reliably determining the tuning parameter presents a significant obstacle, motivating a proliferation of (non-)empirical tuning protocols. A promising recent development is a simplified, effective (ω_{eff}) variant, which ensures high accuracy with minimal numerical effort by circumventing the computationally expensive need for multiple SCF procedures.

The ω_{eff} tuning strategy exhibits markedly improved performance, particularly for systems characterized by charge-transfer (CT) excitations, where it surpasses previously proposed methodologies [117]. Importantly, because this scheme depends exclusively on the electron density, it facilitates the automated execution of RSH calculations for large molecular systems, open-shell radicals, clusters, layered materials, and bulk solids, while remaining free from convergence-related complications [98].

Motivated by these advances, the present work adopts the effective tuning scheme as the starting point for G_0W_0 and BSE calculations of ionization potentials and excitation energies across established benchmark datasets. Furthermore, given that the accurate prediction of semiconductor properties, e.g., optical gaps, continues to pose a significant challenge in nanoscience, stimulating extensive efforts to elucidate the size dependence of these gaps in quantum-confined systems [23, 24, 139], we additionally investigate hydrogenated silicon quantum dots with the new effective tuning scheme.

The paper is organized into four sections. We begin with the methodology, followed by the computational details (Sec. 2). The results and their discussion are presented in (Sec. 3), culminating in a conclusion with perspectives for future work (Sec. 4).

METHODOLOGY AND COMPUTATIONAL DETAILS

To test the accuracy of the effective tuning scheme in G_0W_0 and BSE calculations[31], we have considered a functional with the Coulomb attenuated method (CAM) [140] style partitioning given by

$$\frac{1}{r} = \underbrace{\frac{\alpha + \beta \operatorname{erf}(\omega r)}{r}_{\text{lr}}}_{\text{sr}} + \underbrace{\frac{1 - \alpha - \beta \operatorname{erf}(\omega r)}{r}_{\text{sr}}}_{\text{sr}}, \quad (1)$$

which results in the following form of the XC density functional approximation (DFA)

$$\begin{aligned} E_{xc}(\alpha, \beta; \omega) = & (1 - \alpha)E_x^{\text{srDFA}}(\omega) + \alpha E_x^{\text{srHF}}(\omega) \\ & + [1 - (\alpha + \beta)]E_x^{\text{lrDFA}}(\omega) \\ & + (\alpha + \beta)E_x^{\text{lrHF}}(\omega) + E_c^{\text{DFA}}. \end{aligned} \quad (2)$$

All computations presented herein utilize the LC- ω PBEh[134] functional, a range-separated hybrid (RS) that incorporates the PBE semilocal functional with parameters $\alpha = 0.20$ and $\beta = 0.80$. The specific value of α is motivated by earlier studies that identified the optimal range for this parameter as $0.2 - 0.25$ [65, 101]. Furthermore, this particular DFA was chosen based on its proven capability to enhance the predictive accuracy of many-body perturbation theory calculations, specifically within the G_0W_0 and BSE calculations[80]. The

functional has a relatively high percentage of exact exchange contribution, which was claimed to be crucial for predicting IP within KS[67] and G_0W_0 [11] calculations.

In the assessment, we have chosen three distinct classes of ω tuning schemes, namely

$$\omega = \begin{cases} \omega_{OTRS} = \arg \min_{\omega} (|IP(\omega) + \varepsilon_{\text{HOMO}}(\omega)|^2 + \\ |EA(\omega) + \varepsilon_{\text{LUMO}}(\omega)|^2) \\ \omega_{HOMO} = \arg \min_{\omega} \left| \varepsilon_{\text{HOMO}}^{G_0W_0 @ GKS(\omega)}(\omega) - \varepsilon_{\text{HOMO}}^{GKS(\omega)}(\omega) \right| \\ \omega_{eff} = \frac{a_1}{\langle r_s \rangle} + \frac{a_2 \langle r_s \rangle}{1 + a_3 \langle r_s \rangle^2}. \end{cases} \quad (3)$$

The OTRSH method [65, 101] optimizes the range-separation parameter ω to enforce equality between the HOMO–LUMO gap and the fundamental gap, defined as $IP - EA$, where $IP = E(N-1) - E(N)$ and $EA = E(N) - E(N+1)$. In cases where the anionic state is unbound, the tuning criterion is usually shifted to satisfying Koopmans' theorem (IP tuning).

Beyond OTRSH-tuning, a further refinement known as HOMO tuning[3, 80, 99] has been developed. This method determines the optimal range-separation parameter ω_{HOMO} by finding the value of ω that equalizes the HOMO energy from a G_0W_0 calculation performed on top of $GKS(\omega)$ starting point with the HOMO eigenvalue from that same $GKS(\omega)$ calculation. This matching condition enforces a generalized Koopmans' theorem, ensuring the KS eigenvalue approximates the more accurate quasi-particle energy.

The final expression in Eq. (3) is the effective parameter ω_{eff} , with coefficients $a_1 = 1.91718$, $a_2 = -0.02817$, and $a_3 = 0.14954$. It is defined in terms of the density-weighted Wigner-Seitz radius r_s , whose spatially averaged form is

$$\langle r_s \rangle = \frac{\int \operatorname{erf}\left(\frac{n(\mathbf{r})}{n_c}\right) r_s(\mathbf{r}) d^3r}{\int \operatorname{erf}\left(\frac{n(\mathbf{r})}{n_c}\right) d^3r}, \quad (4)$$

where the weighting is performed using the error function of the density ratio. For a complete derivation, see Ref. [117].

Using the above methodology, we have studied the performance of these tuning schemes in terms of robustness and accuracy in predicting the optical properties on two well-established benchmark datasets and the hydrogenated silicon quantum dots systems using the G_0W_0 and BSE methods. To be more specific, we have considered:

A. The GW100 test set [128]: An IP benchmark comprising 100 small molecules that contains diverse chemical bonds and environments, as it includes different elements. Thus covering a wide range of IPs (from $\sim 4\text{eV}$ (Rb_2) to $\sim 25\text{eV}$ (He)). In this case, all calculations are performed using the def2-TZVPP[133] basis set, and effective core potentials (ECPs) [82] are utilized for heavy

elements. To ensure a rigorous benchmark, we compared our results against high-level CCSD(T) reference IPs [63] and experimental data from Ref. [128]. Because a bound anionic state does not exist for most of these systems, the OTRSH parameter is obtained through IP tuning for all the systems. The ω_{OTRSH} (from IP tuning) and ω_{HOMO} have been taken from Ref. [80].

B. Thiel test set [110, 115]: This comprehensive benchmark provides highly accurate 103 singlet and 63 triplet reference excitation energies for 28 small to medium-sized organic molecules (made of C, N, O, and H elements), including unsaturated aliphatic hydrocarbons, aromatics, heterocycles, carbonyls, amides, and nucleobases. The molecular geometries were taken from Ref. [110]. The TZVP basis set was uniformly adopted for all calculations to ensure direct comparability with the established coupled cluster benchmarks [110]. Although the absence of diffuse functions in this basis set causes convergence problems for the first excitation in ethene and the first bright excitation in pyrrole, this effect is systematic and similarly observed across all computational methods (including CCSD) [10]. The validity of using this basis set is supported in Ref. [10]. Within the set, only hexatriene, benzoquinone, octatetraene, and tetrazine possess a bound anionic state; all other molecules exhibit an unbound anionic state. For these unbound systems, the OTRSH parameter is determined by IP tuning. The range-separated parameters ω_{OTRSH} were taken directly from Ref. [80]. The corresponding ω_{HOMO} value was computed in this work using the LC- ω PBEh functional and the def2-TZVPP basis set using the MOLGW code [12].

C. Hydrogenated Silicon quantum dots (SiQDs): These systems are biocompatible, low-toxicity, and abundant materials[71] with excellent optical properties[15, 33], making them ideal for biomedicine, catalysis, and optoelectronics[125]. Their strong quantum confinement leads to size-dependent variations in IP, HOMO-LUMO gaps, and optical excitation energies. Therefore, SiQDs provide valuable insight into how DFT and MBPT methods capture quasiparticle and excitonic phenomena in confined semiconductor systems. All molecular geometries were optimized in the gas phase using KS-DFT with the B3LYP exchange-correlation functional [5, 68] in conjunction with the cc-pVDZ basis set [29], as implemented in the ORCA software package [86]. The optimized structures were verified to be true local minima by confirming the absence of imaginary frequencies in the harmonic vibrational analysis. Cartesian coordinates of all optimized geometries are provided in the supporting information (SI) file [118]. To manage computational cost, this study analyzes four representative systems (SiH₄, Si₂H₆, Si₅H₁₂, and Si₁₀H₁₆) using the TZVP basis set. To calculate both ω_{OTRSH} (via IP tuning) and ω_{HOMO} for SiQDs LC- ω PBEh/def2-TZVPP in MOLGW was employed. The values for range separation parameters are

provided in the SI.

Finally, the ω_{eff} parameters for all the studies systems have been obtained using PySCF[124] with the script available in the public repository [116]. All G_0W_0 and BSE calculations were performed using the MOLGW code [12]. The computational demands are reduced by employing the resolution of identity (RI) approximation[42] in the Coulomb metric. Furthermore, the frozen core approximation was applied (for the Thiel test set and SiQDs). The visualization of frontier molecular orbitals was performed using the VESTA software package[84].

RESULTS AND DISCUSSIONS

Comparison of ω

Let us first examine the trends in the tuned range-separation parameters ω_{OTRSH} , ω_{HOMO} , and ω_{eff} where the tuning follows Eq. 3, for GW100 set and the Thiel's test set. A comparison among these values is presented in Fig. 1. While the three definitions yield broadly consistent results, notable deviations are observed for certain molecules in the GW100 set, particularly between ω_{OTRSH} (even ω_{HOMO}) and ω_{eff} . Specifically, ω_{OTRSH} spans the range [0.13, 1.00] bohr⁻¹ and ω_{HOMO} lies within [0.13, 0.91] bohr⁻¹, while ω_{eff} remains more narrowly distributed in the range [0.12, 0.47] bohr⁻¹, well within the empirically optimal window of most of the RSH functionals [108]. In general, the ω_{eff} values follow a trend similar to that observed for ω_{OTRSH} and ω_{HOMO} , except for a few cases.

For certain molecules, ω_{OTRSH} reaches unusually large values (0.90-0.99 bohr⁻¹), as observed for 10028-15-6, 12185-09-0, 7440-59-7, and 7783-63-3, corresponding to O₃, P₂, He, and TiF₄, respectively. These cases are characterized by either nearly degenerate frontier orbitals or unbound anionic states, both of which are well known to hinder IP- or HOMO-based tuning schemes [80]. In contrast, ω_{eff} provides physically reasonable values for these cases: 0.298 bohr⁻¹ for O₃, 0.265 bohr⁻¹ for P₂, 0.469 bohr⁻¹ for He and 0.245 bohr⁻¹ for TiF₄.

For systems in Thiel's set the resulting values of ω_{eff} give stable behavior following a trend similar to ω_{OTRSH} and ω_{HOMO} , except for a few cases, where the deviation is larger. Interestingly, for most molecules, the corresponding ω_{eff} average values are found to be approximately 0.3 bohr⁻¹, which is consistent with the optimal range expected for LC-type functionals. This further supports the robustness and general applicability of the effective approach.

TABLE I. Mean signed error (MSE), mean absolute error (MAE), and mean absolute relative error (MARE) for IPs of the $GW100$ set obtained from GKS and G_0W_0 HOMO energies. $GW100$ results are referenced to CCSD(T) values. Full numerical results are available in the SI [118].

Tuning	MSE (eV)	MAE (eV)	MARE (%)
<i>DFT (GKS)</i>			
ω_{eff}	0.32	0.38	3.20
ω_{OTRSH}	-0.11	0.24	2.07
ω_{HOMO}	-0.03	0.14	1.32
<i>MBPT (G_0W_0@GKS)</i>			
ω_{eff}	0.01	0.14	1.34
ω_{OTRSH}	-0.03	0.16	1.47
ω_{HOMO}	-0.02	0.15	1.46

TABLE II. Mean signed error (MSE), mean absolute error (MAE), and mean absolute relative error (MARE) for single (S), tripled (T) excitation energies of Thiel's test set. The Thiel's excitation energies are compared with the theoretical best estimates [110] results. Full numerical results are available in the SI [118].

Method	MSE (eV)	MAE (eV)	MARE (%)
<i>TDDFT (@GKS)</i>			
<i>Singlet</i>			
ω_{eff}	-0.27	0.34	6.30
ω_{OTRSH}	-0.28	0.39	7.33
ω_{HOMO}	-0.22	0.31	5.70
<i>Triplet</i>			
ω_{eff}	0.43	0.49	12.14
ω_{OTRSH}	0.55	0.64	15.47
ω_{HOMO}	0.41	0.49	11.76
<i>Singlet + Triplet</i>			
ω_{eff}	0.08	0.42	9.22
ω_{OTRSH}	0.14	0.52	11.40
ω_{HOMO}	0.10	0.40	8.73
<i>MBPT (BSE@G_0W_0@GKS)</i>			
<i>Singlet</i>			
ω_{eff}	-0.15	0.22	4.17
ω_{OTRSH}	-0.14	0.23	4.30
ω_{HOMO}	-0.11	0.22	4.09
<i>Triplet</i>			
ω_{eff}	0.30	0.40	9.25
ω_{OTRSH}	0.20	0.41	10.28
ω_{HOMO}	0.21	0.40	9.65
<i>Singlet + Triplet</i>			
ω_{eff}	0.08	0.31	6.71
ω_{OTRSH}	0.03	0.32	7.29
ω_{HOMO}	0.05	0.31	6.87

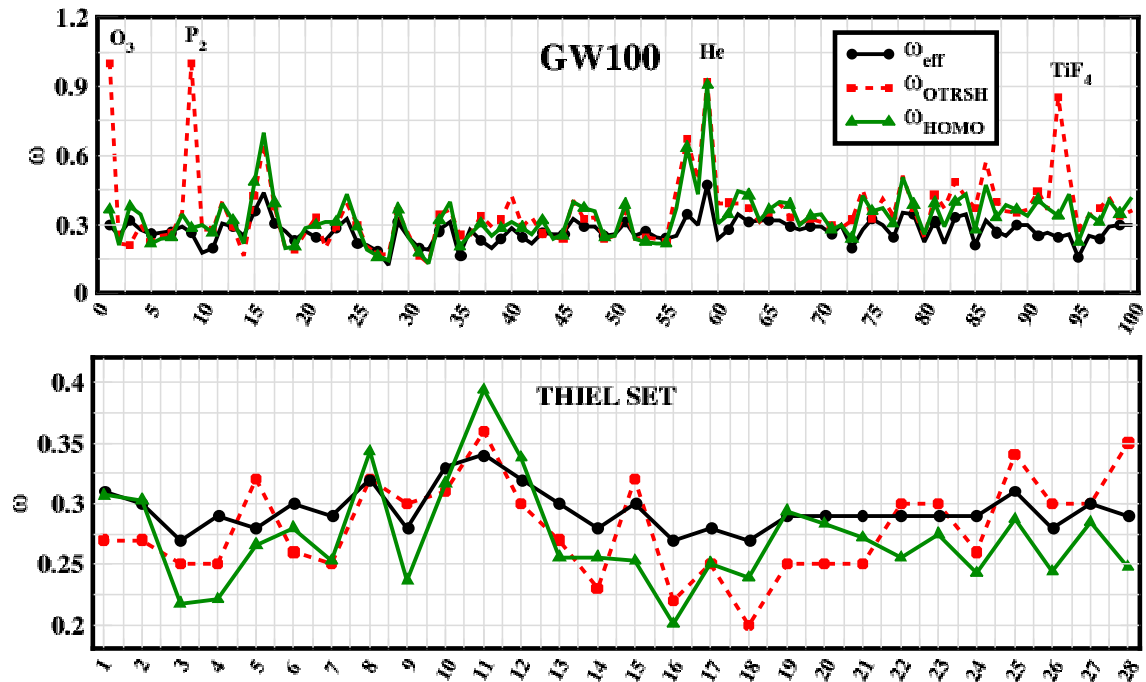


FIG. 1. The figure shows the results of the tuning procedure from Eq. 3, with all parameters given in bohr^{-1} . Results for the GW100 test set are in the top panel, and those for Thiel's set are in the bottom panel. The numbering on the x-axis aligns with the system order listed in Tables S1-S3 of the SI[118].

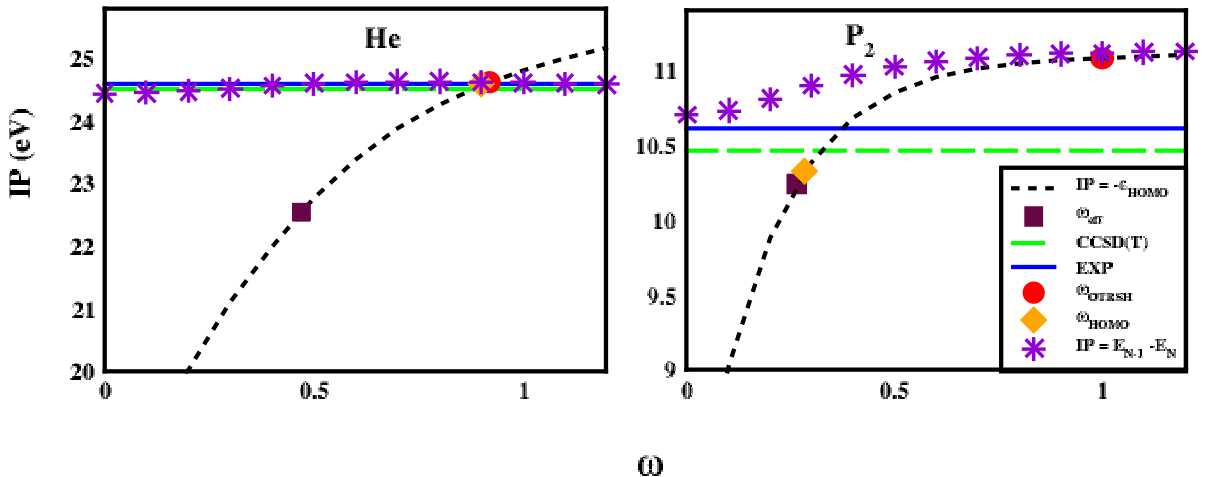


FIG. 2. An illustration of how the variation of ω impacts IP's, we also present the cases where ω_{OTRSH} overestimates the result but ω_{eff} and ω_{HOMO} aligns well with the reference.

Ionization Potential

First, we analyze the performance of various tuning schemes against the GW100 reference IPs, using both the *GKS* and G_0W_0 HOMO orbital energies. Accurate assessment of these IPs is a crucial first step, as the *GKS* and subsequently G_0W_0 corrected eigenvalues provide the essential input for the following BSE calculations.

To this end, in Table I, we compare the impact of tuning scheme on *GKS* and the corresponding G_0W_0 results. Table I summarizes the mean signed errors (MSEs), mean absolute errors (MAEs), and mean absolute relative errors (MAREs) of these predictions computed with respect high-level CCSD(T) reference results. Full results are provided in the SI file [118], including the errors computed relative to experimental values. The corresponding data for the def2-QZVP basis set [133] are also reported

in the SI [118]; the overall trend remains essentially unchanged upon moving to the larger basis set.

One can note that choice of tuning parameter strongly affects the KS-DFT (*GKS*) results, whereas its impact becomes much weaker after applying G_0W_0 corrections. At the KS-DFT (*GKS*) level, ω_{eff} produces the largest and clearly systematic overestimation of the IPs (MSE = 0.32 eV), together with comparatively large absolute errors (MAE = 0.38 eV; MARE = 3.20%). This is not surprising, since the ω_{eff} tuning scheme does not aim to reproduce any particular orbital energy. Nevertheless, as shown in Fig. 2 for He and the P_2 system, effective tuning typically yields fairly accurate IP estimates from the *GKS* HOMO energies compared with other tuning schemes. In contrast, ω_{OTRSH} substantially reduces the bias and improves the overall accuracy (MSE = -0.11 eV; MAE = 0.24 eV; MARE = 2.07%). The best KS-DFT performance is obtained with ω_{HOMO} , which is nearly un-

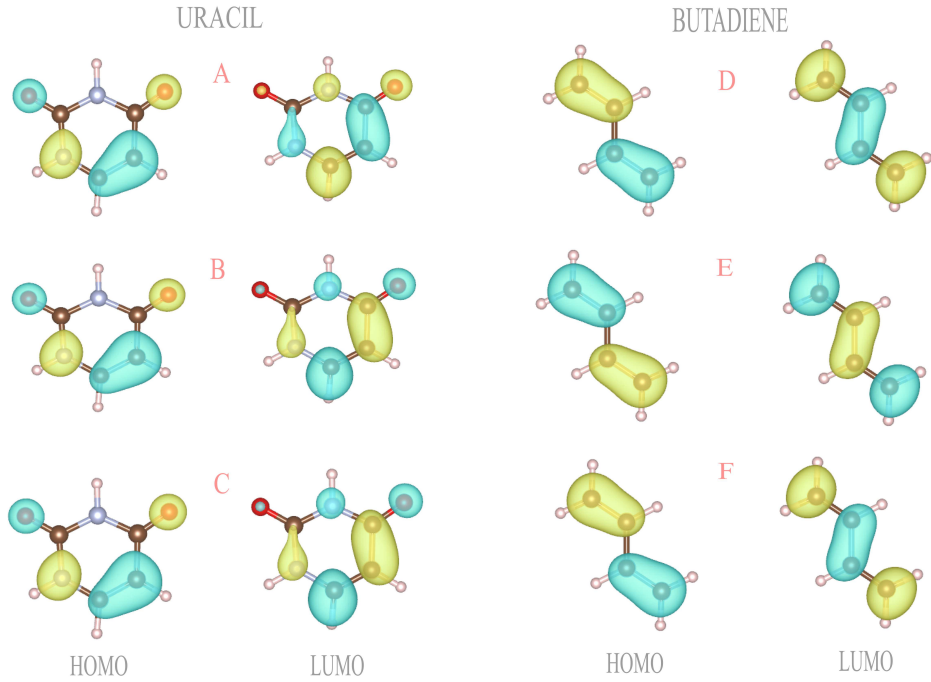


FIG. 3. Visualization of the frontier molecular orbitals (HOMO and LUMO) for Uracil and Butadiene. The plots illustrate the outcomes from three different tuned variants: $GKS(\omega_{eff})$ (A & D), $GKS(\omega_{OTRSH})$ (B & E) and $GKS(\omega_{HOMO})$ (C & F). The def2-TZVPP basis set was used throughout.

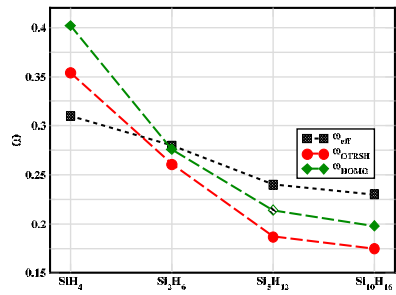


FIG. 4. The range separation parameters ω for few hydrogenated silicon quantum dots (Si_nH_m). The complete data is available in Table S4 of the SI[118].

biased ($MSE = -0.03$ eV) and yields the smallest errors ($MAE = 0.14$ eV; $MARE = 1.32\%$).

To further elucidate the role of the tuning prescription, we analyzed, as a typical example, the real-space distributions of the frontier molecular orbitals of uracil and butadiene. As shown in Fig. 3, the isosurfaces obtained with $GKS(\omega_{eff})$, $GKS(\omega_{OTRSH})$, and $GKS(\omega_{HOMO})$ are qualitatively very similar, indicating that the effective tuning procedure produces orbitals of comparable qual-

ity to the more elaborate multi-SCF ω_{OTRSH} and ω_{HOMO} approaches. An occasional phase inversion is the only minor, visible difference. More importantly, the IPs obtained with ω_{eff} remain comparable in quality with those obtained with other two investigated schemes (see Table S5 in SI file[118]).

Upon moving to MBPT ($G_0W_0@GKS$), the results become very similar across tuning schemes (the MSE is close to zero for all three choices (0.01, -0.03 , and -0.02 eV) leading to very similar values of MAEs (0.14 – 0.16 eV) and MAREs (1.34 – 1.47%). Notably, G_0W_0 dramatically improves the ω_{eff} starting point (MAE reduced from 0.38 to 0.14 eV), indicating that the GW correction largely compensates for the KS-level overestimation. Meanwhile, because ω_{HOMO} already performs very well at the KS-DFT level, the additional G_0W_0 step provides little further benefit and leaves the accuracy essentially unchanged within statistical variation. However, we recall that to obtain the ω_{HOMO} parameter values one requires to perform a complex, multi-step optimization process designed to align the HOMO energies from $G_0W_0@GKS(\omega)$ and $GKS(\omega)$ calculations. For this reason the ω_{HOMO} based IP G_0W_0 results are far more expensive to obtain in comparison to effective tuning counterpart. Thus, the close agreement of all G_0W_0 results underscores the effectiveness of the ω_{eff} scheme as a transferable black-box alternative to the more expensive optimally tuned RSHs.

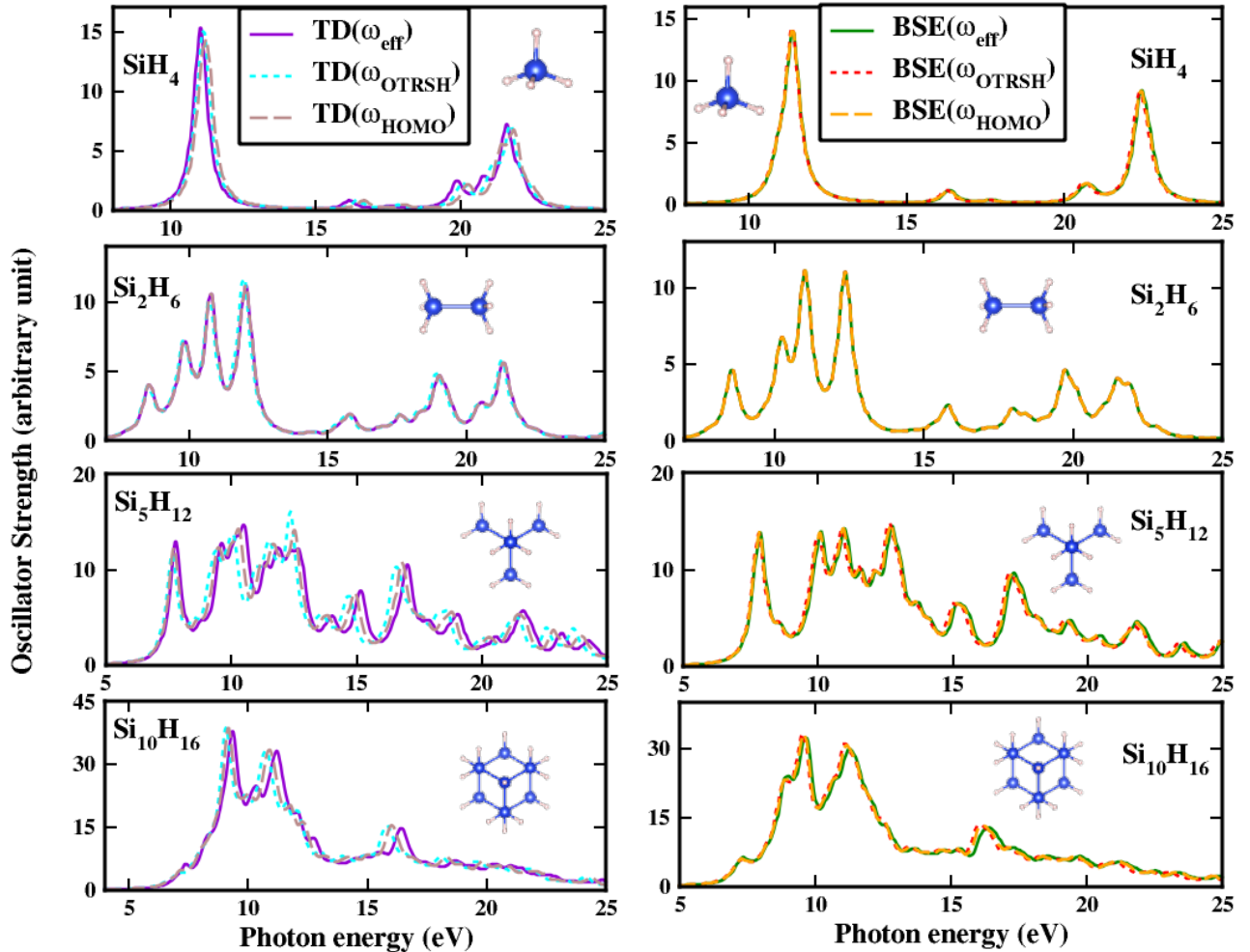


FIG. 5. A comparison of the photoabsorption spectra for silicon clusters calculated with TDDFT (left panel) and the many-body BSE (right panel). The simulations were performed with the LC- ω PBEh functional, considering all RS tuning parameters. The calculations have been performed with TZVP basis set.

Excitation Energies

As a next step, we analyze the excitation energies within the TDDFT and BSE frameworks. Table II summarizes the error statistics for Thiel's test set [110], including both singlet and triplet excitations, where the reference values correspond to the theoretical best estimates (TBE) from Ref. [80]. Within the MBPT framework, the BSE@ G_0W_0 @GKS calculations starting from ω_{eff} based reference perform comparably to those based on the more elaborate ω_{OTRSH} and ω_{HOMO} counterparts. For singlet excitations, the errors obtained for BSE with ω_{eff} (MAE = 0.22 eV, MARE = 4.17%) are nearly identical to those with ω_{OTRSH} (MAE = 0.23 eV, MARE = 4.30%) and ω_{HOMO} (MAE = 0.22 eV, MARE

= 4.09%). Similar trend is observed for triplet BSE excitations energies. Here the ω_{eff} results yield MAE = 0.40 eV and MARE = 9.25% which remain very close to those visible for ω_{OTRSH} (MAE = 0.41 eV, MARE = 10.28%) and ω_{HOMO} (MAE = 0.40 eV, MARE = 9.65%) counterparts. It is noteworthy that ω_{OTRSH} has previously been identified as one of the most accurate starting points for BSE@ G_0W_0 @GKS calculations among a broad range of DFAs [80]. Other commonly used functionals, such as PBE, PBE0, B3LYP, CAM-B3LYP, and BHLYP, generally yield significantly larger MAEs when employed as starting points for BSE@ G_0W_0 @GKS [80]. Therefore, the comparable or even slightly improved performance of the computationally efficient ω_{eff} method highlights its potential as a practical and reliable alternative for generating accurate excitation spectra.

Secondly in Table II we present a comparison of

TDDFT excitation energies calculated using different variants of tuning parameter. Our previous work [117] showed that TDDFT(ω_{eff}) provides enhanced performance for charge-transfer excitations and optical gap predictions in organic photovoltaic (OPV) systems. This advantage persists in the present analysis of Thiel's test set, where both singlet and triplet excitation energies predicted by TDDFT(ω_{eff}) exhibit better agreement with the TBEs compared to TDDFT(ω_{OTRSH}). With accuracy similar to tuned TDDFT(ω_{HOMO}), but without the prohibitive cost of its tuning procedure, which involves expensive multiple G_0W_0 calculations and is not feasible for larger systems. Moreover, traditional DFAs commonly employed in TDDFT calculations [80] generally produce substantially larger MAEs than either of the above tuning variants, reinforcing the importance of incorporating range separation and long-range exchange effects.

Nonetheless, one can see that the adoption of a physically motivated and analytically simple effective range-separation parameter, ω_{eff} , within the RSH framework not only maintains high predictive accuracy but also significantly reduces the computational overhead associated with optimal-tuning procedures. Consequently, the ω_{eff} based RSH approach provides a robust and efficient foundation for both TDDFT and BSE@ G_0W_0 calculations of excitation energies across diverse molecular systems.

Hydrogenated silicon quantum dots

Going beyond molecular systems, the effective range-separation parameter ω_{eff} is also highly relevant for size-dependent nanocrystalline materials. A prototypical example is the family of hydrogenated silicon quantum dots (Si_nH_m), where quantum confinement plays a crucial role in determining their electronic and optical properties. These systems have been extensively studied using a range of theoretical approaches, including DFT, TDDFT, the GW approximation, and BSE [7, 23, 88, 90, 96, 106, 129, 137]. All these studies report strong confinement-induced blue-shifts in the optical gaps and sizable exciton binding energies [88, 90]. Due to the lack of experimental benchmarks for these quantum dots, theoretical predictions from high-level MBPT methods such as GW and BSE [7, 88, 106], as well as from diffusion Monte Carlo (DMC) [7], serve as essential references.

In Fig. 4, we present the size-dependent variation of ω_{eff} for a series of Si_nH_m clusters. Interestingly, ω_{eff} shows a smooth and physically significant trend with respect to cluster size, consistent with previously observed trends [117] and closely tracks the behavior of the IP-based tuning parameter ω_{OTRSH} [123] and ω_{HOMO} . The fact that ω_{eff} nearly approximates ω_{HOMO} (and ω_{OTRSH}), even for relatively large systems, underscores

its practical utility. The direct evaluation of ω_{HOMO} (and ω_{OTRSH}) becomes computationally prohibitive for large clusters, while ω_{eff} offers a viable and less demanding alternative (see Table S4 in SI file).

Table III presents the calculated HOMO, HOMO-LUMO gaps, optical gaps, and exciton binding energies obtained from different tuning protocols. The results from both TDDFT and MBPT are internally consistent. With increasing cluster size, the HOMO becomes less negative and both the HOMO-LUMO gap and the optical gap E_{opt} decrease. In parallel, the exciton binding energy E_{ex} decreases systematically (from ~ 6 eV to ~ 4 eV), consistent with weaker electron-hole binding and enhanced screening in larger clusters. At the TDDFT level, the tuning protocol introduces a noticeable spread in gaps and excitation energies. Overall, ω_{OTRSH} tends to yield slightly larger HOMO-LUMO gaps and E_{opt} than ω_{HOMO} , while ω_{eff} typically provides intermediate values, i.e., a compromise between the more gap-opening OTRSH tuning and the more gap-reducing HOMO-based tuning. This behavior suggests that ω_{eff} balances the effective range of exchange in a way that moderates both quasiparticle-like gaps and excitonic effects within TDDFT. In contrast, MBPT results are only weakly dependent on the underlying tuning choice, including ω_{eff} , with variations typically limited to a few hundredths to at most ~ 0.1 eV. This indicates that quasiparticle corrections (G_0W_0) and the explicit electron-hole interaction (BSE) largely mitigate starting-point differences introduced by the tuned functional. Comparison with DMC optical gaps shows that TDDFT and BSE@ G_0W_0 generally overestimate E_{opt} for the smallest cluster, but the discrepancy decreases with size; for $Si_{10}H_{16}$ the calculated optical gaps approach the DMC reference. Overall, Table III suggests that tuning primarily affects TDDFT predictions, whereas BSE@ G_0W_0 provides more robust, less protocol-dependent optical gaps, and that ω_{eff} behaves as a stable tuning strategy.

Expanding the analysis, Table IV reports the optical absorption energies of SiH_4 and Si_2H_6 , two systems for which reliable experimental reference data are available. For both clusters, the TDDFT results obtained with the ω_{eff} parameter are consistently more accurate, showing closer agreement with experiment than those computed using ω_{OTRSH} or ω_{HOMO} . The same trend holds for the BSE calculations: although BSE generally overestimates excitation energies, the overestimation is substantially reduced when ω_{eff} is used in place of ω_{OTRSH} or ω_{HOMO} .

Figure 5 compares the corresponding optical spectra from TDDFT (left) and BSE (right) using the three tuning protocols. In TDDFT (left panel), the spectra differ only modestly, with noticeable changes limited to a subset of features. By contrast, the BSE spectra (right panel) display a clear, peak-by-peak correspondence across the three parameter choices, indicating a stronger sensitivity of the BSE peak positions to the tun-

TABLE III. HOMO, HOMO-LUMO gaps, optical gaps, and exciton binding energies using different tuning protocols for *TDDFT* and *MBPT* variants are presented. All energies are in eV. Diffusion quantum Monte Carlo (DMC) results from ref. [7, 137]

Cluster Property	DFT/TDDFT			G ₀ W ₀ /BSE			DMC
	ω_{eff}	ω_{OTRSH}	ω_{HOMO}	ω_{eff}	ω_{OTRSH}	ω_{HOMO}	
SiH ₄	HOMO	-12.50	-13.11	-12.97	-12.71	-12.77	-12.75
	$E_{HOMO-LUMO}$	15.72	16.56	16.37	16.45	16.53	16.51
	E_{ex}	6.11	6.64	6.53	6.56	6.54	6.54
	E_{opt}	9.61	9.92	9.84	9.89	9.99	9.97
Si ₂ H ₆	HOMO	-10.66	-10.98	-10.66	-10.39	-10.43	-10.39
	$E_{HOMO-LUMO}$	13.04	13.54	13.04	13.30	13.37	13.30
	E_{ex}	5.29	5.67	5.29	5.51	5.53	5.51
	E_{opt}	7.75	7.87	7.75	7.79	7.84	7.79
Si ₅ H ₁₂	HOMO	-10.07	-10.15	-9.90	-9.67	-9.68	-9.64
	$E_{HOMO-LUMO}$	11.61	11.75	11.34	11.67	11.69	11.63
	E_{ex}	4.73	4.84	4.52	4.70	4.71	4.69
	E_{opt}	6.88	6.91	6.82	6.97	6.98	6.94
Si ₁₀ H ₁₆	HOMO	-9.80	-9.75	-9.53	-9.15	-9.15	-9.11
	$E_{HOMO-LUMO}$	10.31	10.24	9.89	9.97	9.96	9.89
	E_{ex}	4.13	4.08	3.84	3.86	3.86	3.84
	E_{opt}	6.18	6.16	6.05	6.11	6.10	6.05

TABLE IV. Optical absorption energies (in eV) for SiH₄ and Si₂H₆ using different tuning protocols for GKS and G₀W₀ variants. Experimental (Expt) values are taken from [50].

Cluster	Expt	TDDFT (@GKS)			MBPT (BSE@G ₀ W ₀ @GKS)		
		ω_{eff}	ω_{OTRSH}	ω_{HOMO}	ω_{eff}	ω_{OTRSH}	ω_{HOMO}
SiH ₄	8.80	9.61	9.92	9.84	9.89	9.99	9.97
	9.70	9.85	10.17	10.09	10.16	10.26	10.23
	10.70	10.70	10.82	11.02	10.80	10.88	10.86
Si ₂ H ₆	7.60	7.75	7.87	7.75	7.79	7.85	7.60
	8.40	8.55	8.72	8.55	8.58	8.63	8.40
	9.50	9.29	9.51	9.29	9.64	9.71	9.50
	9.90	9.67	10.01	9.67	9.93	10.00	9.90

ing procedure.

Overall, these results show that ω_{eff} not only captures the correct size dependence of key observables, but also provides a computationally efficient and physically well-motivated choice for describing electronic excitations in nanostructured materials.

CONCLUSION

In this work, we have systematically assessed the performance of a recently proposed, physically motivated, and computationally efficient range-separation tuning strategy for RSH functionals in the context of many-body perturbation theory methods. Specifically, we demonstrated that the effective screening parameter ω_{eff} , derived from the average electron density, serves as a robust, transferable and much computationally accessible alternative to conventional tuning schemes based on the ionization potential theorem or HOMO alignment.

By employing ω_{eff} within an RSH framework as the starting point for single-shot G₀W₀ and BSE calculations, we achieved ionization potentials and excitation

energies in excellent agreement with high-level reference data for the GW100 set and Thiel's benchmark test set. Notably, the accuracy of G₀W₀@GKS(ω_{eff}) matches that of optimally tuned functionals, yet it completely avoids their demanding, multi step tuning procedure. Although the ω_{HOMO} approach may appear slightly more accurate in some cases, this comes again with a substantial computational burden. Furthermore, for a series of hydrogenated silicon nanoclusters (Si_{*n*}H_{*m*}), we showed that ω_{eff} captures the expected size-dependent trends and yields optical gaps and exciton binding energies consistent with those from diffusion Monte Carlo and BSE calculations. This highlights the applicability of ω_{eff} beyond molecular systems, making it a practical tool for exploring excited-state properties in nanoscale and extended materials.

Overall, our results indicate that GKS(ω_{eff}) serves as a physically justified, black-box replacement for standard tuning methods, offering a dependable initial setup for G₀W₀ and BSE computations while considerably lowering the computational cost. This method is especially advantageous for large-scale and high-throughput investigations, in which conventional tuning approaches become impractical.

Notably, the effective tuning strategy has recently been adopted to predict charge-transfer processes more accurately than wavefunction theory, supporting the design of efficient dye-sensitized solar cells based on organic dyes.[119]. Similar applications of the effective-tuning protocol are being actively pursued in our group, and the corresponding results will be reported in due course.

ACKNOWLEDGEMENTS

S.Ś. acknowledges the financial support from the National Science Centre, Poland (grant no. 2021/42/E/ST4/00096).

* aditisin gh4812@doktorant.umk.pl

† szs miga@fizyka.umk.pl

- [1] Stefan Albrecht, Lucia Reining, Rodolfo Del Sole, et al. Ab Initio Calculation of Excitonic Effects in the Optical Spectra of Semiconductors. *Phys. Rev. Lett.*, 80:4510–4513, May 1998. URL: <https://link.aps.org/doi/10.1103/PhysRevLett.80.4510>, doi:10.1103/PhysRevLett.80.4510.
- [2] E. Aprá, E. J. Bylaska, W. A. de Jong, et al. NWChem: Past, present, and future. *The Journal of Chemical Physics*, 152(18):184102, 05 2020. doi:10.1063/5.004997.
- [3] Viktor Atalla, Mina Yoon, Fabio Caruso, et al. Hybrid density functional theory meets quasiparticle calculations: A consistent electronic structure approach. *Phys. Rev. B*, 88:165122, Oct 2013. URL: <https://link.aps.org/doi/10.1103/PhysRevB.88.165122>, doi:10.1103/PhysRevB.88.165122.
- [4] Roi Baer, Ester Livshits, and Ulrike Salzner. Tuned Range-Separated Hybrids in Density Functional Theory. *Annual Review of Physical Chemistry*, 61(Volume 61, 2010):85–109, 2010. URL: <https://www.annualreviews.org/content/journals/10.1146/annurev.physchem.012809.103321>, doi:10.1146/annurev.physchem.012809.103321.
- [5] Axel D Becke. Density-functional thermochemistry. III. The role of exact exchange. *J. Chem. Phys.*, 98(7):5648–5652, 1993.
- [6] Mauro Del Ben, Charlene Yang, Zhenglu Li, et al. Accelerating large-scale excited-state GW calculations on leadership HPC systems. In *Proceedings of the International Conference for High Performance Computing, Networking, Storage and Analysis*, SC ’20. IEEE Press, 2020.
- [7] Lorin X. Benedict, Aaron Puzder, Andrew J. Williamson, et al. Calculation of optical absorption spectra of hydrogenated Si clusters: Bethe-Salpeter equation versus time-dependent local-density approximation. *Phys. Rev. B*, 68:085310, Aug 2003. URL: <https://link.aps.org/doi/10.1103/PhysRevB.68.085310>, doi:10.1103/PhysRevB.68.085310.
- [8] Xavier Blase, Ivan Duchemin, Denis Jacquemin, et al. The Bethe-Salpeter Equation Formalism: From Physics to Chemistry. *The Journal of Physical Chemistry Letters*, 11(17):7371–7382, 2020. doi:10.1021/acs.jpclett.0c01875.
- [9] Fabien Bruneval, Nike Dattani, and Michiel J. van Setten. The GW Miracle in Many-Body Perturbation Theory for the Ionization Potential of Molecules. *Frontiers in Chemistry*, 9, 2021. URL: <https://www.frontiersin.org/journals/chemistry/articles/10.3389/fchem.2021.749779>, doi:10.3389/fchem.2021.749779.
- [10] Fabien Bruneval, Samia M. Hamed, and Jeffrey B. Neaton. A systematic benchmark of the ab initio Bethe-Salpeter equation approach for low-lying optical excitations of small organic molecules. *The Journal of Chemical Physics*, 142(24):244101, 06 2015. doi:10.1063/1.4922489.
- [11] Fabien Bruneval and Miguel A. L. Marques. Benchmarking the Starting Points of the GW Approximation for Molecules. *Journal of Chemical Theory and Computation*, 9(1):324–329, 2013. doi:10.1021/ct300835h.
- [12] Fabien Bruneval, Tonatiuh Rangel, Samia M. Hamed, et al. molgw 1: Many-body perturbation theory software for atoms, molecules, and clusters. *Computer Physics Communications*, 208:149–161, 2016. URL: <https://www.sciencedirect.com/science/article/pii/S0010465516301990>, doi:10.1016/j.cpc.2016.06.019.
- [13] Fabien Bruneval, Nathalie Vast, and Lucia Reining. Effect of self-consistency on quasiparticles in solids. *Phys. Rev. B*, 74:045102, Jul 2006. URL: <https://link.aps.org/doi/10.1103/PhysRevB.74.045102>, doi:10.1103/PhysRevB.74.045102.
- [14] Kieron Burke. Perspective on density functional theory. *J. Chem. Phys.*, 136(15):150901, 2012.
- [15] L. T. Canham. Silicon quantum wire array fabrication by electrochemical and chemical dissolution of wafers. *Applied Physics Letters*, 57(10):1046–1048, 09 1990. arXiv:https://pubs.aip.org/aip/apl/article-pdf/57/10/1046/18478329/1046_1_online.pdf, doi:10.1063/1.103561.
- [16] Fabio Caruso, Patrick Rinke, Xinguo Ren, et al. Self-consistent GW: All-electron implementation with localized basis functions. *Phys. Rev. B*, 88:075105, Aug 2013. URL: <https://link.aps.org/doi/10.1103/PhysRevB.88.075105>, doi:10.1103/PhysRevB.88.075105.
- [17] MARK E. CASIDA. *Time-Dependent Density Functional Response Theory for Molecules*, pages 155–192.
- [18] Mark E. Casida, Christine Jamorski, Kim C. Casida, et al. Molecular excitation energies to high-lying bound states from time-dependent density-functional response theory: Characterization and correction of the time-dependent local density approximation ionization threshold. *The Journal of Chemical Physics*, 108(11):4439–4449, 03 1998. doi:10.1063/1.475855.
- [19] M.E. Casida and M. Huix-Rotllant. Progress in Time-Dependent Density-Functional Theory. *Annual Review of Physical Chemistry*, 63(Volume 63, 2012):287–323, 2012.
- [20] Wei Chen, Giacomo Miceli, Gian-Marco Rignanese, et al. Nonempirical dielectric-dependent hybrid functional with range separation for semiconductors and insulators. *Phys. Rev. Mater.*, 2:073803, Jul 2018.
- [21] Yeongsu Cho, Sylvia J. Bintrim, and Timothy C. Berkelbach. Simplified GW/BSE Approach for Charged and Neutral Excitation Energies of Large Molecules and Nanomaterials. *Journal of Chemical Theory and Computation*, 18(6):3438–3446, 2022. doi:10.1021/acs.jctc.2c00087.
- [22] Brian Cunningham. Many-body theory beyond GW: Towards a complete description of two-body correlated propagation. *Phys. Rev. Res.*, 6:043277, Dec 2024. URL: <https://link.aps.org/doi/10.1103/PhysRevResearch.6.043277>, doi:10.1103/PhysRevResearch.6.043277.

[23] C. Delerue, M. Lannoo, and G. Allan. Excitonic and Quasiparticle Gaps in Si Nanocrystals. *Phys. Rev. Lett.*, 84:2457–2460, Mar 2000. URL: <https://link.aps.org/doi/10.1103/PhysRevLett.84.2457>, doi:10.1103/PhysRevLett.84.2457.

[24] B. Delley and E. F. Steigmeier. Quantum confinement in Si nanocrystals. *Phys. Rev. B*, 47:1397–1400, Jan 1993. URL: <https://link.aps.org/doi/10.1103/PhysRevB.47.1397>, doi:10.1103/PhysRevB.47.1397.

[25] Jack Deslippe, Georgy Samsonidze, David A. Strubbe, et al. BerkeleyGW: A massively parallel computer package for the calculation of the quasiparticle and optical properties of materials and nanostructures. *Computer Physics Communications*, 183(6):1269–1289, 2012. URL: <https://www.sciencedirect.com/science/article/pii/S0010465511003912>, doi:10.1016/j.cpc.2011.12.006.

[26] Andreas Dreuw, Jennifer L. Weisman, and Martin Head-Gordon. Long-range charge-transfer excited states in time-dependent density functional theory require non-local exchange. *The Journal of Chemical Physics*, 119(6):2943–2946, 08 2003. doi:10.1063/1.1590951.

[27] Ivan Duchemin and Xavier Blase. Cubic-Scaling All-Electron GW Calculations with a Separable Density-Fitting Space-Time Approach. *Journal of Chemical Theory and Computation*, 17(4):2383–2393, 2021. doi:10.1021/acs.jctc.1c00101.

[28] Ivan Duchemin, Denis Jacquemin, and Xavier Blase. Combining the GW formalism with the polarizable continuum model: A state-specific non-equilibrium approach. *The Journal of Chemical Physics*, 144(16):164106, 04 2016. doi:10.1063/1.4946778.

[29] Jr. Dunning, Thom H. Gaussian basis sets for use in correlated molecular calculations. I. The atoms boron through neon and hydrogen. *J. Chem. Phys.*, 90(2):1007–1023, 01 1989.

[30] Marc Dvorak, Dorothea Golze, and Patrick Rinke. Quantum embedding theory in the screened Coulomb interaction: Combining configuration interaction with *GW/BSE*. *Phys. Rev. Mater.*, 3:070801, Jul 2019. URL: <https://link.aps.org/doi/10.1103/PhysRevMaterials.3.070801>, doi:10.1103/PhysRevMaterials.3.070801.

[31] C. Faber, P. Boulanger, C. Attaccalite, et al. Excited states properties of organic molecules: from density functional theory to the *GW* and Bethe-Salpeter Green's function formalisms. *Philosophical Transactions of the Royal Society A: Mathematical, Physical and Engineering Sciences*, 372(2011):20130271, 2014. URL: <https://royalsocietypublishing.org/doi/abs/10.1098/rsta.2013.0271>, doi:10.1098/rsta.2013.0271.

[32] F. Fuchs, J. Furthmüller, F. Bechstedt, et al. Quasiparticle band structure based on a generalized Kohn-Sham scheme. *Phys. Rev. B*, 76:115109, Sep 2007. URL: <https://link.aps.org/doi/10.1103/PhysRevB.76.115109>, doi:10.1103/PhysRevB.76.115109.

[33] Shoji Furukawa and Tatsuro Miyasato. Three-dimensional quantum well effects in ultrafine silicon particles. *Japanese Journal of Applied Physics*, 27(11A):L2207, nov 1988. doi:10.1143/JJAP.27.L2207.

[34] Stephen E. Gant, Jonah B. Haber, Marina R. Filip, et al. Optimally tuned starting point for single-shot *GW* calculations of solids. *Phys. Rev. Mater.*, 6:053802, May 2022. URL: <https://link.aps.org/doi/10.1103/PhysRevMaterials.6.053802>.

[35] Weiwei Gao, Zhao Tang, Jijun Zhao, et al. Efficient Full-Frequency GW Calculations Using a Lanczos Method. *Phys. Rev. Lett.*, 132:126402, Mar 2024. URL: <https://link.aps.org/doi/10.1103/PhysRevLett.132.126402>, doi:10.1103/PhysRevLett.132.126402.

[36] Arghya Ghosh, Subrata Jana, Dimple Rani, et al. Accurate and efficient prediction of the band gaps and optical spectra of chalcopyrite semiconductors from a nonempirical range-separated dielectric-dependent hybrid: Comparison with many-body perturbation theory. *Phys. Rev. B*, 109:045133, Jan 2024. URL: <https://link.aps.org/doi/10.1103/PhysRevB.109.045133>, doi:10.1103/PhysRevB.109.045133.

[37] Soumen Ghosh, Pragya Verma, Christopher J. Cramer, et al. Combining Wave Function Methods with Density Functional Theory for Excited States. *Chemical Reviews*, 118(15):7249–7292, 2018. doi:10.1021/acs.chemrev.8b00193.

[38] Andrew T. B. Gilbert, Nicholas A. Besley, and Peter M. W. Gill. Self-Consistent Field Calculations of Excited States Using the Maximum Overlap Method (MOM). *The Journal of Physical Chemistry A*, 112(50):13164–13171, 2008. doi:10.1021/jp801738f.

[39] Dorothea Golze, Marc Dvorak, and Patrick Rinke. The GW Compendium: A Practical Guide to Theoretical Photoemission Spectroscopy. *Frontiers in Chemistry*, 7, 2019. URL: <https://www.frontiersin.org/articles/10.3389/fchem.2019.00377>, doi:10.3389/fchem.2019.00377.

[40] Lars Hedin. New Method for Calculating the One-Particle Green's Function with Application to the Electron-Gas Problem. *Phys. Rev.*, 139:A796–A823, Aug 1965. URL: <https://link.aps.org/doi/10.1103/PhysRev.139.A796>, doi:10.1103/PhysRev.139.A796.

[41] Lars Hedin. On correlation effects in electron spectroscopies and the GW approximation. *Journal of Physics: Condensed Matter*, 11(42):R489, oct 1999. URL: <https://dx.doi.org/10.1088/0953-8984/11/42/201>, doi:10.1088/0953-8984/11/42/201.

[42] Mario Hernández Vera and Thomas-C. Jagau. Resolution-of-the-identity approximation for complex-scaled basis functions. *The Journal of Chemical Physics*, 151(11):111101, 09 2019. arXiv:https://pubs.aip.org/aip/jcp/article-pdf/doi/10.1063/1.5119695/13540625/111101_1_online.pdf, doi:10.1063/1.5119695.

[43] Jochen Heyd and Gustavo E. Scuseria. Efficient hybrid density functional calculations in solids: Assessment of the Heyd-Scuseria-Ernzerhof screened Coulomb hybrid functional. *J. Chem. Phys.*, 121(3):1187–1192, 2004.

[44] Jochen Heyd, Gustavo E Scuseria, and Matthias Ernzerhof. Hybrid functionals based on a screened Coulomb potential. *J. Chem. Phys.*, 118(18):8207–8215, 2003.

[45] So Hirata and Martin Head-Gordon. Time-dependent density functional theory within the Tamm-Danoff approximation. *Chemical Physics Letters*, 314(3):291–299, 1999. URL: <https://www.sciencedirect.com/science/article/pii/S0009261499011495>, doi:10.1016/S0009-2614(99)01149-5.

[46] Daichi Hirose, Yoshifumi Noguchi, and Osamu Sugino. All-electron $GW +$ Bethe-Salpeter calculations on small molecules. *Phys. Rev. B*, 91:205111, May 2015. URL: <https://link.aps.org/doi/10.1103/PhysRevB.91.205111>, doi:10.1103/PhysRevB.91.205111.

[47] Falco Hüser, Thomas Olsen, and Kristian S. Thygesen. Quasiparticle GW calculations for solids, molecules, and two-dimensional materials. *Phys. Rev. B*, 87:235132, Jun 2013. URL: <https://link.aps.org/doi/10.1103/PhysRevB.87.235132>, doi:10.1103/PhysRevB.87.235132.

[48] Mark S. Hybertsen and Steven G. Louie. First-Principles Theory of Quasiparticles: Calculation of Band Gaps in Semiconductors and Insulators. *Phys. Rev. Lett.*, 55:1418–1421, Sep 1985. URL: <https://link.aps.org/doi/10.1103/PhysRevLett.55.1418>, doi:10.1103/PhysRevLett.55.1418.

[49] Mark S. Hybertsen and Steven G. Louie. Electron correlation in semiconductors and insulators: Band gaps and quasiparticle energies. *Phys. Rev. B*, 34:5390–5413, Oct 1986. URL: <https://link.aps.org/doi/10.1103/PhysRevB.34.5390>, doi:10.1103/PhysRevB.34.5390.

[50] Uichi Itoh, Yasutake Toyoshima, Hideo Onuki, et al. Vacuum ultraviolet absorption cross sections of SiH₄, GeH₄, Si₂H₆, and Si₃H₈. *The Journal of Chemical Physics*, 85(9):4867–4872, 11 1986. doi:10.1063/1.451721.

[51] Subrata Jana, Arghya Ghosh, Lucian A. Constantin, et al. Simple and effective screening parameter for range-separated dielectric-dependent hybrids. *Phys. Rev. B*, 108:045101, Jul 2023. URL: <https://link.aps.org/doi/10.1103/PhysRevB.108.045101>, doi:10.1103/PhysRevB.108.045101.

[52] Subrata Jana, Abhilash Patra, Lucian A. Constantin, et al. Long-range screened hybrid-functional theory satisfying the local-density linear response. *Phys. Rev. A*, 99:042515, Apr 2019.

[53] Subrata Jana, Abhilash Patra, Lucian A. Constantin, et al. Screened range-separated hybrid by balancing the compact and slowly varying density regimes: Satisfaction of local density linear response. *J. Chem. Phys.*, 152(4):044111, 2020.

[54] Subrata Jana, Abhilash Patra, and Prasanjit Samal. Efficient lattice constants and energy bandgaps for condensed systems from a meta-GGA level screened range-separated hybrid functional. *The Journal of Chemical Physics*, 149(9):094105, 09 2018. doi:10.1063/1.5037030.

[55] Subrata Jana, Bikash Patra, Szymon Śmiga, et al. Improved solid stability from a screened range-separated hybrid functional by satisfying semiclassical atom theory and local density linear response. *Phys. Rev. B*, 102:155107, Oct 2020.

[56] Subrata Jana and Prasanjit Samal. A meta-GGA level screened range-separated hybrid functional by employing short range Hartree-Fock with a long range semilocal functional. *Phys. Chem. Chem. Phys.*, 20:8999–9005, 2018.

[57] Subrata Jana and Prasanjit Samal. Screened hybrid meta-GGA exchange-correlation functionals for extended systems. *Phys. Chem. Chem. Phys.*, 21:3002–3015, 2019. URL: <http://dx.doi.org/10.1039/C8CP06715E>, doi:10.1039/C8CP06715E.

[58] Hong Jiang, Ricardo I. Gomez-Abal, Patrick Rinke, et al. Localized and Itinerant States in Lanthanide Oxides United by $GW @ LDA + U$. *Phys. Rev. Lett.*, 102:126403, Mar 2009. URL: <https://link.aps.org/doi/10.1103/PhysRevLett.102.126403>, doi:10.1103/PhysRevLett.102.126403.

[59] Siriluk Kanchanakungwankul and Donald G. Truhlar. Examination of How Well Long-Range-Corrected Density Functionals Satisfy the Ionization Energy Theorem. *Journal of Chemical Theory and Computation*, 17(8):4823–4830, 2021. doi:10.1021/acs.jctc.1c00440.

[60] Andreas Karolewski, Leeor Kronik, and Stephan Kümmel. Using optimally tuned range separated hybrid functionals in ground-state calculations: Consequences and caveats. *The Journal of Chemical Physics*, 138(20):204115, 05 2013. doi:10.1063/1.4807325.

[61] Emmanouil Kioupakis, Peihong Zhang, Marvin L. Cohen, et al. GW quasiparticle corrections to the LDA + UGGA + U electronic structure of bcc hydrogen. *Phys. Rev. B*, 77:155114, Apr 2008. URL: <https://link.aps.org/doi/10.1103/PhysRevB.77.155114>, doi:10.1103/PhysRevB.77.155114.

[62] Joseph W. Knight, Xiaopeng Wang, Lukas Gallandi, et al. Accurate Ionization Potentials and Electron Affinities of Acceptor Molecules III: A Benchmark of GW Methods. *Journal of Chemical Theory and Computation*, 12(2):615–626, 2016. doi:10.1021/acs.jctc.5b00871.

[63] Katharina Krause, Michael E. Harding, and Wim Klopper. Coupled-cluster reference values for the GW27 and GW100 test sets for the assessment of GW methods. *Molecular Physics*, 113(13–14):1952–1960, 2015. doi:10.1080/00268976.2015.1025113.

[64] Leeor Kronik and Stephan Kümmel. Dielectric Screening Meets Optimally Tuned Density Functionals. *Advanced Materials*, 30(41):1706560, 2018.

[65] Leeor Kronik, Tamar Stein, Sivan Refael-Y Abramson, et al. Excitation Gaps of Finite-Sized Systems from Optimally Tuned Range-Separated Hybrid Functionals. *Journal of Chemical Theory and Computation*, 8(5):1515–1531, 2012.

[66] Aliaksandr V Krukau, Oleg A Vydrov, Artur F Izmaylov, et al. Influence of the exchange screening parameter on the performance of screened hybrid functionals. *J. Chem. Phys.*, 125(22):224106, 2006.

[67] Vignesh Balaji Kumar, Szymon Śmiga, and Ireneusz Grabowski. A critical evaluation of the hybrid ks dft functionals based on the ks exchange-correlation potentials. *The Journal of Physical Chemistry Letters*, 15(40):10219–10229, 2024. PMID: 39356205. arXiv: <https://doi.org/10.1021/acs.jpclett.4c01979>, doi:10.1021/acs.jpclett.4c01979.

[68] Chengteh Lee, Weitao Yang, and Robert G Parr. Development of the Colle-Salvetti correlation-energy formula into a functional of the electron density. *Phys. Rev. B*, 37(2):785, 1988.

[69] Xia Leng, Fan Jin, Min Wei, et al. GW method and *Bethe – Salpeter* equation for calculating electronic excitations. *WIREs Computational Molecular Science*, 6(5):532–550, 2016. doi:10.1002/wcms.1265.

[70] Je-Luen Li, G.-M. Rignanese, and Steven G. Louie. Quasiparticle energy bands of NiO in the GW approximation. *Phys. Rev. B*, 71:193102, May 2005.

URL: <https://link.aps.org/doi/10.1103/PhysRevB.71.193102>, doi:10.1103/PhysRevB.71.193102.

[71] Ruonan Li, Jian Xu, Xiqiong Mu, and Fankui Zeng. A comprehensive review on the synthesis methods and applications of silicon quantum dots (sqds). *Next Nanotechnology*, 7:100144, 2025. URL: <https://www.sciencedirect.com/science/article/pii/S2949829525000130>, doi:10.1016/j.nxnano.2025.100144.

[72] Chi Liu, Jan Kloppenburg, Yi Yao, et al. All-electron ab initio Bethe-Salpeter equation approach to neutral excitations in molecules with numeric atom-centered orbitals. *The Journal of Chemical Physics*, 152(4):044105, 01 2020. doi:10.1063/1.5123290.

[73] Peitao Liu, Merzuk Kaltak, Ji ří Klimeš, et al. Cubic scaling *GW*: Towards fast quasiparticle calculations. *Phys. Rev. B*, 94:165109, Oct 2016. URL: <https://link.aps.org/doi/10.1103/PhysRevB.94.165109>, doi:10.1103/PhysRevB.94.165109.

[74] Steven G. Louie and Mark S. Hybertsen. Theory of quasiparticle energies: Band gaps and excitation spectra in solids. *International Journal of Quantum Chemistry*, 32(S21):31–44, 1987. doi:10.1002/qua.560320706.

[75] Steven G. Louie and Angel Rubio. *Quasiparticle and Optical Properties of Solids and Nanostructures: The GW-BSE Approach*, pages 215–240. Springer Netherlands, Dordrecht, 2005. URL: <https://doi.org/10.1007/978-1-4020-3286-8%5F12>, doi:10.1007/978-1-4020-3286-8_12.

[76] Neepa T. Maitra. Perspective: Fundamental aspects of time-dependent density functional theory. *The Journal of Chemical Physics*, 144(22):220901, 06 2016. doi:10.1063/1.4953039.

[77] Noa Marom, Fabio Caruso, Xinguo Ren, et al. Benchmark of *GW* methods for azabzenes. *Phys. Rev. B*, 86:245127, Dec 2012. URL: <https://link.aps.org/doi/10.1103/PhysRevB.86.245127>, doi:10.1103/PhysRevB.86.245127.

[78] Margherita Marsili, Alejandro Molina-Sánchez, Maurizia Palummo, et al. Spinorial formulation of the *GW*-BSE equations and spin properties of excitons in two-dimensional transition metal dichalcogenides. *Phys. Rev. B*, 103:155152, Apr 2021. URL: <https://link.aps.org/doi/10.1103/PhysRevB.103.155152>, doi:10.1103/PhysRevB.103.155152.

[79] Margherita Marsili, Edoardo Mosconi, Filippo De Angelis, et al. Large-scale *GW*-BSE calculations with N^3 scaling: Excitonic effects in dye-sensitized solar cells. *Phys. Rev. B*, 95:075415, Feb 2017. URL: <https://link.aps.org/doi/10.1103/PhysRevB.95.075415>, doi:10.1103/PhysRevB.95.075415.

[80] Caroline A. McKeon, Samia M. Hamed, Fabien Bruneval, et al. An optimally tuned range-separated hybrid starting point for ab initio *GW* plus Bethe-Salpeter equation calculations of molecules. *The Journal of Chemical Physics*, 157(7):074103, 08 2022. doi:10.1063/5.0097582.

[81] Daniel Mejia-Rodriguez, Alexander Kunitsa, Edoardo Aprá, et al. Scalable Molecular *GW* Calculations: Valence and Core Spectra. *Journal of Chemical Theory and Computation*, 17(12):7504–7517, 2021. doi:10.1021/acs.jctc.1c00738.

[82] William E. III Minnette, Erik P. Hoy, and Andrew M. Sand. The use of effective core potentials with multi-configuration pair-density functional theory. *The Journal of Physical Chemistry A*, 128(31):6555–6565, 2024. PMID: 39052857. arXiv:<https://doi.org/10.1021/acs.jpca.4c02666>, doi:10.1021/acs.jpca.4c02666.

[83] Takashi Miyake, Peihong Zhang, Marvin L. Cohen, et al. Quasiparticle energy of semicore d electrons in ZnS: Combined LDA + U and *GW* approach. *Phys. Rev. B*, 74:245213, Dec 2006. URL: <https://link.aps.org/doi/10.1103/PhysRevB.74.245213>, doi:10.1103/PhysRevB.74.245213.

[84] Koichi Momma and Fujio Izumi. *VESTA*: a three-dimensional visualization system for electronic and structural analysis. *Journal of Applied Crystallography*, 41(3):653–658, Jun 2008.

[85] Paula Mori-Sánchez, Aron J. Cohen, and Weitao Yang. Localization and Delocalization Errors in Density Functional Theory and Implications for Band-Gap Prediction. *Phys. Rev. Lett.*, 100:146401, Apr 2008. URL: <https://link.aps.org/doi/10.1103/PhysRevLett.100.146401>, doi:10.1103/PhysRevLett.100.146401.

[86] F. Neese. Software update: the orca program system, version 5.0. *WIRES Comput. Molec. Sci.*, 12(1):e1606, 2022.

[87] Daniel Neuhauser, Yi Gao, Christopher Arntsen, et al. Breaking the Theoretical Scaling Limit for Predicting Quasiparticle Energies: The Stochastic *GW* Approach. *Phys. Rev. Lett.*, 113:076402, Aug 2014. URL: <https://link.aps.org/doi/10.1103/PhysRevLett.113.076402>, doi:10.1103/PhysRevLett.113.076402.

[88] Serdar Öğüt, James R. Chelikowsky, and Steven G. Louie. Optical Properties of Silicon Nanocrystals: A First Principles Study. *MRS Online Proceedings Library*, 579(1):81–89, Dec 1999. doi:10.1557/PROC-579-81.

[89] Guy Ohad, Dahyvd Wing, Stephen E. Gant, et al. Band gaps of halide perovskites from a Wannier-localized optimally tuned screened range-separated hybrid functional. *Phys. Rev. Mater.*, 6:104606, Oct 2022.

[90] Serdar Öğüt, James R. Chelikowsky, and Steven G. Louie. Quantum Confinement and Optical Gaps in Si Nanocrystals. *Phys. Rev. Lett.*, 79:1770–1773, Sep 1997. URL: <https://link.aps.org/doi/10.1103/PhysRevLett.79.1770>, doi:10.1103/PhysRevLett.79.1770.

[91] Giovanni Onida, Lucia Reining, and Angel Rubio. Electronic excitations: density-functional versus many-body Green's-function approaches. *Rev. Mod. Phys.*, 74:601–659, Jun 2002. URL: <https://link.aps.org/doi/10.1103/RevModPhys.74.601>, doi:10.1103/RevModPhys.74.601.

[92] Maurizia Palummo, Conor Hogan, Francesco Sottile, et al. Ab initio electronic and optical spectra of free-base porphyrins: The role of electronic correlation. *The Journal of Chemical Physics*, 131(8):084102, 08 2009. doi:10.1063/1.3204938.

[93] RamÃşn L. Panadés-Barrueta and Dorothea Golze. Accelerating Core-Level *GW* Calculations by Combining the Contour Deformation Approach with the Analytic Continuation of W . *Journal of Chemical Theory and Computation*, 19(16):5450–5464, 2023. doi:10.1021/acs.jctc.3c00555.

[94] John P. Perdew and Mel Levy. Physical Content of the Exact Kohn-Sham Orbital Energies: Band Gaps and Derivative Discontinuities. *Phys. Rev. Lett.*, 51:1884–1887, Nov 1983. URL: <https://link.aps.org/doi/10.1103/PhysRevLett.51.1884>, doi:10.1103/PhysRevLett.51.1884.

[95] Antonio Prlj, Basile F. E. Curchod, Alberto Fabrizio, et al. Qualitatively Incorrect Features in the TDDFT Spectrum of Thiophene-Based Compounds. *The Journal of Physical Chemistry Letters*, 6(1):13–21, 2015. doi:10.1021/jz5022087.

[96] Aaron Puzder, A. J. Williamson, Jeffrey C. Grossman, et al. Surface Chemistry of Silicon Nanoclusters. *Phys. Rev. Lett.*, 88:097401, Feb 2002. URL: <https://link.aps.org/doi/10.1103/PhysRevLett.88.097401>, doi:10.1103/PhysRevLett.88.097401.

[97] Tonatiuh Rangel, Mauro Del Ben, Daniele Varsano, et al. Reproducibility in G_0W_0 calculations for solids. *Computer Physics Communications*, 255:107242, 2020. URL: <https://www.sciencedirect.com/science/article/pii/S0010465520300734>, doi:10.1016/j.cpc.2020.107242.

[98] Tonatiuh Rangel, Samia M. Hamed, Fabien Bruneval, et al. Evaluating the GW Approximation with CCSD(T) for Charged Excitations Across the Oligoacenes. *Journal of Chemical Theory and Computation*, 12(6):2834–2842, 2016. doi:10.1021/acs.jctc.6b00163.

[99] Tonatiuh Rangel, Samia M. Hamed, Fabien Bruneval, et al. An assessment of low-lying excitation energies and triplet instabilities of organic molecules with an ab initio Bethe-Salpeter equation approach and the Tamm-Dancoff approximation. *The Journal of Chemical Physics*, 146(19):194108, 05 2017. doi:10.1063/1.4983126.

[100] Sivan Refael-Abramson, Diana Y. Qiu, Steven G. Louie, et al. Defect-Induced Modification of Low-Lying Excitons and Valley Selectivity in Monolayer Transition Metal Dichalcogenides. *Phys. Rev. Lett.*, 121:167402, Oct 2018. URL: <https://link.aps.org/doi/10.1103/PhysRevLett.121.167402>, doi:10.1103/PhysRevLett.121.167402.

[101] Sivan Refael-Abramson, Sahar Sharifzadeh, Niranjan Govind, et al. Quasiparticle Spectra from a Nonempirical Optimally Tuned Range-Separated Hybrid Density Functional. *Phys. Rev. Lett.*, 109:226405, Nov 2012. URL: <https://link.aps.org/doi/10.1103/PhysRevLett.109.226405>, doi:10.1103/PhysRevLett.109.226405.

[102] Lucia Reining. The GW approximation: content, successes and limitations. *WIREs Computational Molecular Science*, 8(3):e1344, 2018. doi:10.1002/wcms.1344.

[103] Xinguo Ren, Florian Merz, Hong Jiang, et al. All-electron periodic G_0W_0 implementation with numerical atomic orbital basis functions: Algorithm and benchmarks. *Phys. Rev. Mater.*, 5:013807, Jan 2021. URL: <https://link.aps.org/doi/10.1103/PhysRevMaterials.5.013807>, doi:10.1103/PhysRevMaterials.5.013807.

[104] Xinguo Ren, Patrick Rinke, Volker Blum, et al. Resolution-of-identity approach to Hartree-Fock, hybrid density functionals, RPA, MP2 and GW with numeric atom-centered orbital basis functions. *New Journal of Physics*, 14(5):053020, may 2012. URL: <https://dx.doi.org/10.1088/1367-2630/14/5/053020>, doi:10.1088/1367-2630/14/5/053020.

[105] Ryan M. Richard, Michael S. Marshall, O. Dolgo-unitcheva, et al. Accurate Ionization Potentials and Electron Affinities of Acceptor Molecules I. Reference Data at the CCSD(T) Complete Basis Set Limit. *Journal of Chemical Theory and Computation*, 12(2):595–604, 2016. doi:10.1021/acs.jctc.5b00875.

[106] Michael Rohlfing and Steven G. Louie. Excitonic Effects and the Optical Absorption Spectrum of Hydrogenated Si Clusters. *Phys. Rev. Lett.*, 80:3320–3323, Apr 1998. URL: <https://link.aps.org/doi/10.1103/PhysRevLett.80.3320>, doi:10.1103/PhysRevLett.80.3320.

[107] Michael Rohlfing and Steven G. Louie. Electron-hole excitations and optical spectra from first principles. *Phys. Rev. B*, 62:4927–4944, Aug 2000. URL: <https://link.aps.org/doi/10.1103/PhysRevB.62.4927>, doi:10.1103/PhysRevB.62.4927.

[108] Mary A. Rohrdanz, Katie M. Martins, and John M. Herbert. A long-range-corrected density functional that performs well for both ground-state properties and time-dependent density functional theory excitation energies, including charge-transfer excited states. *The Journal of Chemical Physics*, 130(5):054112, 2009.

[109] Nora Salas-Illanes, Dmitrii Nabok, and Claudia Draxl. Electronic structure of representative band-gap materials by all-electron quasiparticle self-consistent GW calculations. *Phys. Rev. B*, 106:045143, Jul 2022. URL: <https://link.aps.org/doi/10.1103/PhysRevB.106.045143>, doi:10.1103/PhysRevB.106.045143.

[110] Marko Schreiber, Mario R. Silva-Junior, Stephan P. A. Sauer, et al. Benchmarks for electronically excited states: CASPT2, CC2, CCSD, and CC3. *The Journal of Chemical Physics*, 128(13):134110, 04 2008. doi:10.1063/1.2889385.

[111] L. J. Sham and M. Schlüter. Density-Functional Theory of the Energy Gap. *Phys. Rev. Lett.*, 51:1888–1891, Nov 1983. URL: <https://link.aps.org/doi/10.1103/PhysRevLett.51.1888>, doi:10.1103/PhysRevLett.51.1888.

[112] Manas Sharma and Marek Sierka. Optical Gaps of Ionic Materials from GW/BSE-in-DFT and CC2-in-DFT. *Journal of Chemical Theory and Computation*, 20(21):9592–9605, 2024. doi:10.1021/acs.jctc.4c00819.

[113] M. Shishkin and G. Kresse. Self-consistent GW calculations for semiconductors and insulators. *Phys. Rev. B*, 75:235102, Jun 2007. URL: <https://link.aps.org/doi/10.1103/PhysRevB.75.235102>, doi:10.1103/PhysRevB.75.235102.

[114] M. Shishkin, M. Marsman, and G. Kresse. Accurate Quasiparticle Spectra from Self-Consistent GW Calculations with Vertex Corrections. *Phys. Rev. Lett.*, 99:246403, Dec 2007. URL: <https://link.aps.org/doi/10.1103/PhysRevLett.99.246403>, doi:10.1103/PhysRevLett.99.246403.

[115] Mario R. Silva-Junior, Marko Schreiber, Stephan P. A. Sauer, et al. Benchmarks of electronically excited states: Basis set effects on CASPT2 results. *The Journal of Chemical Physics*, 133(17):174318, 11 2010. doi:10.1063/1.3499598.

[116] Aditi Singh. Tuned range separated made simple, 2025. <https://github.com/aditisinha4812/>

`simplified_tuned_range_separated`.

[117] Aditi Singh, Subrata Jana, Lucian A. Constantin, et al. Simplified, Physically Motivated, and Broadly Applicable Range-Separation Tuning. *The Journal of Physical Chemistry Letters*, 16(32):8198–8208, 2025. doi: 10.1021/acs.jpclett.5c01441.

[118] Aditi Singh, Subrata Jana, and Szymon Śmiga. Simplified range-separation tuning as a practical starting point for g_0w_0 and bethe-salpeter calculations, January 2026. Additional data, computational details, and extended results.

[119] Aditi Singh, Ram Dhari Pandey, Subrata Jana, Prasanjit Samal, Paweł Tecmer, and Szymon Śmiga. A simplified approach for modulating frontier orbitals of prototypical organic dyes for efficient dye-sensitized solar cells. Manuscript submitted for publication, January 2026. Under review at *Journal of Chemical Theory and Computation*.

[120] Szymon Śmiga, Volodymyr Marusiak, Ireneusz Grabowski, et al. The ab initio density functional theory applied for spin-polarized calculations. *The Journal of Chemical Physics*, 152(5):054109, 02 2020. doi:10.1063/1.5128933.

[121] Monika Srebro and Jochen Autschbach. Tuned Range-Separated Time-Dependent Density Functional Theory Applied to Optical Rotation. *Journal of Chemical Theory and Computation*, 8(1):245–256, 2012. doi: 10.1021/ct200764g.

[122] Adrian Stan, Nils Erik Dahlen, and Robert van Leeuwen. Levels of self-consistency in the GW approximation. *The Journal of Chemical Physics*, 130(11):114105, 03 2009. doi:10.1063/1.3089567.

[123] Tamar Stein, Helen Eisenberg, Leeor Kronik, et al. Fundamental Gaps in Finite Systems from Eigenvalues of a Generalized Kohn-Sham Method. *Phys. Rev. Lett.*, 105:266802, Dec 2010.

[124] Qiming Sun, Xing Zhang, Samragni Banerjee, et al. Recent developments in the PySCF program package. *The Journal of Chemical Physics*, 153(2):024109, 07 2020. doi:10.1063/5.0006074.

[125] H. Takagi, H. Ogawa, Y. Yamazaki, A. Ishizaki, and T. Nakagiri. Quantum size effects on photoluminescence in ultrafine si particles. *Applied Physics Letters*, 56(24):2379–2380, 06 1990. arXiv:https://pubs.aip.org/aip/apl/article-pdf/56/24/2379/18476967/2379_1_online.pdf, doi:10.1063/1.102921.

[126] Murilo L. Tiago, Sohrab Ismail-Beigi, and Steven G. Louie. Effect of semicore orbitals on the electronic band gaps of Si, Ge, and GaAs within the GW approximation. *Phys. Rev. B*, 69:125212, Mar 2004. URL: <https://link.aps.org/doi/10.1103/PhysRevB.69.125212>, doi:10.1103/PhysRevB.69.125212.

[127] M. J. van Setten, M. Giantomassi, X. Gonze, et al. Automation methodologies and large-scale validation for GW: Towards high-throughput GW calculations. *Phys. Rev. B*, 96:155207, Oct 2017. URL: <https://link.aps.org/doi/10.1103/PhysRevB.96.155207>, doi:10.1103/PhysRevB.96.155207.

[128] Michiel J. van Setten, Fabio Caruso, Sahar Sharifzadeh, et al. GW100: Benchmarking G0W0 for Molecular Systems. *Journal of Chemical Theory and Computation*, 11(12):5665–5687, 2015. doi:10.1021/acs.jctc.5b00453.

[129] Igor Vasiliev, Serdar Öğüt, and James R. Chelikowsky. Ab Initio Absorption Spectra and Optical Gaps in Nanocrystalline Silicon. *Phys. Rev. Lett.*, 86:1813–1816, Feb 2001. URL: <https://link.aps.org/doi/10.1103/PhysRevLett.86.1813>, doi:10.1103/PhysRevLett.86.1813.

[130] J. Villalobos-Castro, Iryna Knysh, Denis Jacquemin, et al. Lagrangian Z-vector approach to Bethe-Salpeter analytic gradients: Assessing approximations. *The Journal of Chemical Physics*, 159(2):024116, 07 2023. doi:10.1063/5.0156687.

[131] Vojtěch Vlček, Wenfei Li, Roi Baer, et al. Swift GW beyond 10,000 electrons using sparse stochastic compression. *Phys. Rev. B*, 98:075107, Aug 2018. URL: <https://link.aps.org/doi/10.1103/PhysRevB.98.075107>, doi:10.1103/PhysRevB.98.075107.

[132] Vojtěch Vlček, Eran Rabani, Daniel Neuhauser, et al. Stochastic GW Calculations for Molecules. *Journal of Chemical Theory and Computation*, 13(10):4997–5003, 2017. doi:10.1021/acs.jctc.7b00770.

[133] Florian Weigend and Reinhart Ahlrichs. Balanced basis sets of split valence, triple zeta valence and quadruple zeta valence quality for h to rn: Design and assessment of accuracy. *Phys. Chem. Chem. Phys.*, 7:3297–3305, 2005. URL: <http://dx.doi.org/10.1039/B508541A>, doi:10.1039/B508541A.

[134] Elon Weintraub, Thomas M. Henderson, and Gustavo E. Scuseria. Long-Range-Corrected Hybrids Based on a New Model Exchange Hole. *Journal of Chemical Theory and Computation*, 5(4):754–762, 2009. doi: 10.1021/ct800530u.

[135] Ming Wen, Vibin Abraham, Gaurav Harsha, et al. Comparing Self-Consistent GW and Vertex-Corrected G_0W_0 ($G_0W_0\Gamma$) Accuracy for Molecular Ionization Potentials. *Journal of Chemical Theory and Computation*, 20(8):3109–3120, 2024. doi:10.1021/acs.jctc.3c01279.

[136] Jan Wilhelm, Patrick Seewald, and Dorothea Golze. Low-Scaling GW with Benchmark Accuracy and Application to Phosphorene Nanosheets. *Journal of Chemical Theory and Computation*, 17(3):1662–1677, 2021. doi:10.1021/acs.jctc.0c01282.

[137] Andrew J. Williamson, Jeffrey C. Grossman, Randolph Q. Hood, et al. Quantum Monte Carlo Calculations of Nanostructure Optical Gaps: Application to Silicon Quantum Dots. *Phys. Rev. Lett.*, 89:196803, Oct 2002. URL: <https://link.aps.org/doi/10.1103/PhysRevLett.89.196803>, doi:10.1103/PhysRevLett.89.196803.

[138] Dahyvd Wing, Guy Ohad, Jonah B. Haber, et al. Band gaps of crystalline solids from Wannier-localization-based optimal tuning of a screened range-separated hybrid functional. *Proceedings of the National Academy of Sciences*, 118(34):e2104556118, 2021. doi:10.1073/pnas.2104556118.

[139] M. V. Wolkin, J. Jorne, P. M. Fauchet, et al. Electronic States and Luminescence in Porous Silicon Quantum Dots: The Role of Oxygen. *Phys. Rev. Lett.*, 82:197–200, Jan 1999. URL: <https://link.aps.org/doi/10.1103/PhysRevLett.82.197>, doi:10.1103/PhysRevLett.82.197.

[140] Takeshi Yanai, David P Tew, and Nicholas C Handy. A new hybrid exchange-correlation functional using the Coulomb-attenuating method (CAM-

B3LYP). *Chemical Physics Letters*, 393(1):51–57, 2004. URL: <https://www.sciencedirect.com/science/article/pii/S0009261404008620>, doi: 10.1016/j.cplett.2004.06.011.

[141] Linyao Zhang, Yinan Shu, Chang Xing, et al. Recommendation of Orbitals for G0W0 Calculations on Molecules and Crystals. *Journal of Chemical Theory and Computation*, 18(6):3523–3537, 2022. doi: 10.1021/acs.jctc.2c00242.

[142] Yan Zhao and Donald G. Truhlar. Density Functional for Spectroscopy: No Long-Range Self-Interaction Error, Good Performance for Rydberg and Charge-Transfer States, and Better Performance on Average than B3LYP for Ground States. *The Journal of Physical Chemistry A*, 110(49):13126–13130, 2006. doi: 10.1021/jp066479k.